

# Weak Radar Signal Detection Based on Variable Band Selection

**JONG-WOO SHIN**, Member, IEEE  
Pusan National University  
Busan, Republic of Korea

**KYU-HA SONG**  
Agency for Defense Development  
Daejeon, Republic of Korea

**KYOUNG-SIK YOON**  
**HYOUNG-NAM KIM**, Member, IEEE  
Pusan National University  
Busan, Republic of Korea

**Electronic warfare support (ES) plays an important role in gathering and analyzing signals from enemy emitters to provide friendly electronic attack (EA) systems or electronic protection (EP) systems with crucial information. However, ES systems may have difficulty in gathering meaningful signals because there is no prior information about the signal in most cases, and the signal is sometimes too weak or distorted. In this paper, we propose a novel weak-signal detection method to solve these problems based on a modified sinc wavelet transform. This method exploits the frequency shifting property to change the center frequency of a band-pass filter and then applies the scaling property of the continuous-time wavelet transform to vary its bandwidth. This approach is distinguished from previous works in terms of the detection capability of weak signals with high-frequency or multifrequency components. Computer simulation results show that the proposed method can be used in practical implementation to deal with signals that have a low signal-to-noise ratio (SNR).**

Manuscript received February 15, 2015; revised August 23, 2015, December 11, 2015; released for publication February 25, 2016.

DOI: No. 10.1109/TAES.2016.150121.

Refereeing of this contribution was handled by P. Pace.

This research was supported by Agency for Defense Development (ADD), Korea under Contract UD150003ED.

Part of this work has been published in the *Proceedings of Military Communications Conference (MILCOM)*, Boston, MA, 2009 [27].

Authors' addresses: J.-W. Shin, K.-S. Yoon, H.-N. Kim, Department of Electronics Engineering, Pusan National University, Busan 609-735, Republic of Korea; K.-H. Song, Agency for Defense Development, Daejeon 305-152, Republic of Korea. Corresponding author is H.-N. Kim, E-mail: (hnmkim@pusan.ac.kr).

0018-9251/16/\$26.00 © 2016 IEEE

## I. INTRODUCTION

In modern warfare, much electronic equipment is used to carry out various tasks, and the application areas have steadily increased. This trend has increased the importance of electronic warfare (EW), which is the art and science of preserving the use of the electromagnetic spectrum for friendly forces while denying its use to the enemy. Naturally, the development of proper countermeasures has also accelerated [1–5].

EW has commonly been classified into three subfields according to the operations: electronic warfare support (ES), electronic attack (EA), and electronic protection (EP). ES systems collect and analyze signals from enemy emitters and then provide processed information to friendly EA and EP systems. Successful acquisition of the information is a prerequisite for accomplishing the duties of EA and EP systems and is directly linked to issues of a battle [1, 6].

To protect friendly forces from enemy threats, all threatening radar signals should be carefully detected and analyzed. Unfortunately, detecting target signals becomes more and more difficult in complicated EW environments for various reasons. First, it is impossible to obtain prior information such as the frequency band and direction of signals from enemy emitters. Second, the radar signal is easily distorted by various disturbances such as noise and channel conditions. Third, many types of emitters are also operated simultaneously to search for and track unidentified objects in modern warfare. The various signals also make it difficult to extract a desired target signal. Finally, gathering enemy radar signals is generally performed from long distances, resulting in huge power attenuation due to free-path loss.

These problems are directly linked to the detection performance of ES systems. To stably secure a weak radar signal, robust signal acquisition methods that can be applied in very noisy environments are essential. There have been various studies to cope with the problems that occur in ES systems, but they have mainly focused on pulse train separation and radar identification while assuming that the received radar signal is quite clean [7–14]. Although important, these studies have seldom dealt with fundamental issues like noise reduction for better performance of the receivers in ES systems.

To develop a method for detecting weak radar signals, several de-noising methods have been proposed [15–19]. Band-pass filters have been employed for de-noising after finding out the operating frequency of the radar signal [1]. However, when enemies try to keep radar signal information secret by changing the operating frequency, such a filtering process becomes almost useless. Approaches based on the continuous wavelet transform (CWT) have received considerable attention for removing noise signals in the field of image processing [16, 18]. However, there have not been many cases applied in radar signal processing. Owing to its multiresolution time and frequency properties, CWT can be used effectively to

reduce noise signals in cases of unknown weak radar signals.

This paper focuses on the detection of a weak signal based on CWT, which can be used to maximize the signal-to-noise ratio (SNR) of a received weak signal by adjusting the scaling factor. Although CWT has been used to find weak radar signals in several studies [8, 10, 16], the methods work only when the receiver already has information about the enemy radar signals. Since the detection performance of these methods cannot be guaranteed for radar signals with high frequency or multiple frequencies, we introduce a new mother wavelet based on a sinc function and apply a frequency shift property to solve these problems. The mother wavelet is a principal function that characterizes the basic wavelet shape. Due to the admissibility [8], the sinc function itself originally cannot be a mother wavelet. However, we found that the frequency-shifted mother wavelet, which has a flat frequency gain and variable passband characteristic, qualifies a sinc function as a mother wavelet. As a result, the proposed method is able to select the frequency band and can be applied to the detection of unknown weak radar signals by suppressing the noise signal. In addition, we also describe a way to set initial values in the proposed method.

The rest of this paper is organized as follows. In Section II, we briefly describe the CWT and analyze the conventional method to detect a radar signal with weak power. Section III presents the noise reduction method to support the weak signal detection. Section IV presents the performance evaluation of the proposed method through computer simulations. Finally, Section V concludes the paper.

## II. NOISE REDUCTION PROBLEM IN ELECTRONIC WARFARE SUPPORT SYSTEMS

### A. Electronic Warfare Support Systems

The overall operation of the ES system is shown in Fig. 1. Using a broad omni-directional antenna, the receiver collects various signals from hidden enemy emitters. After receiving signals, ES systems measure signal parameters such as the operating frequency, pulse amplitude (PA), pulsewidth (PW), time of arrival (TOA), and pulse repetition interval (PRI). If there are several radar signals at the same time, they are separated into independent pulse trains by signal analysis of the pattern and correlativity. The measured parameters of the isolated pulse streams are compared with a database of characteristics stored in the emitter library, and then ES systems identify the emitter type, such as a search or tracking radar. Finally, ES systems report meaningful information to friendly EP and EA systems [20].

For an effective ES system, parameters of the received signal should be accurately estimated, and a signal with high SNR should be provided. However, it is difficult for ES systems to secure high-power signals. Since the reception process is similar to that of a passive radar,

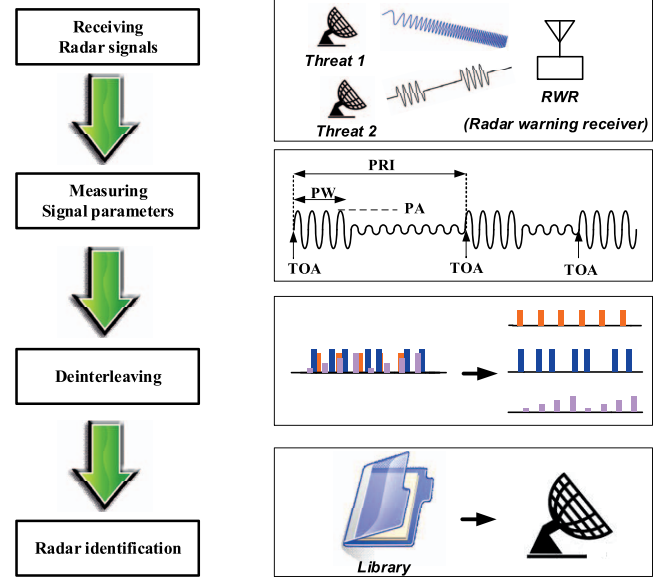


Fig. 1. Functional block diagram for radar identification from unknown radar signals in ES system.

friendly ES systems just receive wideband signals passively in a designated area.

### B. Wavelet-Based Noise Reduction Method

The basic idea of the CWT is to decompose the original signal into a series of transformed signals through scaling and translation [21]. The transformed signals have different levels of time and frequency resolution. These properties come from the dilating operation of a principal function called a mother wavelet. Based on these characteristics, the CWT makes it possible to determine the local time and frequency characteristics of the original signal and to enhance the SNR of the original signal by analyzing these characteristics. Thus, CWT-based noise reduction could be more promising than traditional de-noising methods such as low-pass or band-pass filtering mapped from the Fourier transform (FT) when applied to frequently encountered situations of nonstationary signals in EW systems.

The CWT is basically represented by the inner products of a signal  $f(t)$  and the translated and dilated wavelet  $\Psi_{s,b}(t)$  as follows [22, 23]:

$$\begin{aligned} W(s, b) &\equiv \int_{-\infty}^{\infty} f(t) \psi_{s,b}^*(t) dt \\ &\equiv \int_{-\infty}^{\infty} f(t) \frac{1}{\sqrt{|s|}} \psi^* \left( \frac{t-b}{s} \right) dt, \end{aligned} \quad (1)$$

where

$$\psi_{s,b}(t) = \frac{1}{\sqrt{|s|}} \cdot \psi \left( \frac{t-b}{s} \right) \quad (2)$$

and  $s$  is a scaling factor and  $b$  is a time shift. The CWT in (1) can be represented with a convolution operator  $*$  as follows [22]:

$$W(s, b) = f(b) * \psi_{s,0}^*(-b). \quad (3)$$

From (3), the CWT can be regarded as equivalent to the output of a filter with an impulse response  $\psi_{s,0}^*(-b)$  and an input  $f(b)$  for any given scaling factor  $s$ . The impulse response  $\psi_{s,0}^*(-b)$  operates as a band-pass filter with bandwidth that varies according to the scaling factor. This filter suppresses other undesired signal components while maintaining the desired target signal if an appropriate scaling factor is chosen. This means that the CWT can effectively support detection of weak radar signals.

To obtain the optimal scaling factor, we define the output SNR after CWT as an amplitude ratio between the squared integral of the wavelet transformed original signal and that of the wavelet transformed noise signal. In a set of  $L$  candidates of scaling factors  $\{s_1, s_2, \dots, s_L\}$ , the optimal scaling factor  $s_{\text{opt}}$  is determined by a value that produces the maximum SNR after transformation. Thus, the optimal scaling factor is determined by [8, 16]

$$s_{\text{opt}} = \arg \max_{s \in \{s_1, s_2, \dots, s_L\}} \left\{ \frac{\int_{-\infty}^{\infty} |W_{\text{signal}}(s, b)|^2 db}{E \left[ \int_{-\infty}^{\infty} |W_{\text{noise}}(s, b)|^2 db \right]} \right\} \quad (4)$$

where  $E[\cdot]$  is an expectation operator and  $\arg \max_x f(x)$  is the value of  $x$  at which the maximum of  $f(x)$  is attained. Previous work on a CWT-based noise-reduction method [16] used computer simulation to find an optimal scaling factor with a Gaussian mother wavelet in a low-SNR situation. The method succeeded in finding a square wave (baseband signal) when the SNR was  $-10$  dB. However, this method may not provide the same performance when detecting unknown weak radar signals if there is no prior information about the signals. To consider a square wave, the received signal should be demodulated to the baseband signal with prior information on the operating frequency. However, ES systems do not generally have prior knowledge of the received signal, so the acquisition of a baseband signal may be hard or impractical. In this situation, detection performance may not be ensured.

To analyze the frequency characteristics of the previous method [16], the frequency-domain characteristics of the wavelet transform are shown in Fig. 2. This figure shows the time-domain waveforms and the frequency responses of widely used mother wavelets (Gaussian, Morlet, and Mexican hat). These mother wavelets do not show flat gain in the frequency domain and thus cannot be directly applied for detecting a weak radar signal without prior knowledge of the signal spectrum.

Several examples are illustrated in Fig. 3 for a Gaussian wavelet. Let  $\Psi_{s,0}^*(f)$ ,  $N(f)$ , and  $S(f)$  be FTs of  $\psi_{s,0}^*(-b)$ , a certain realization of additive white Gaussian noise (AWGN), and an input radar signal  $s(b)$ , respectively. In Fig. 3, changing the scaling factor produces variation in the bandwidth and the magnitude of  $\Psi_{s,0}^*(f)$ . Specifically, when  $s > 1$ , the bandwidth shrinks while the magnitude increases, as shown in Fig. 3(b). In Fig. 3(c), the bandwidth increases and the magnitude decreases for  $s < 1$ .

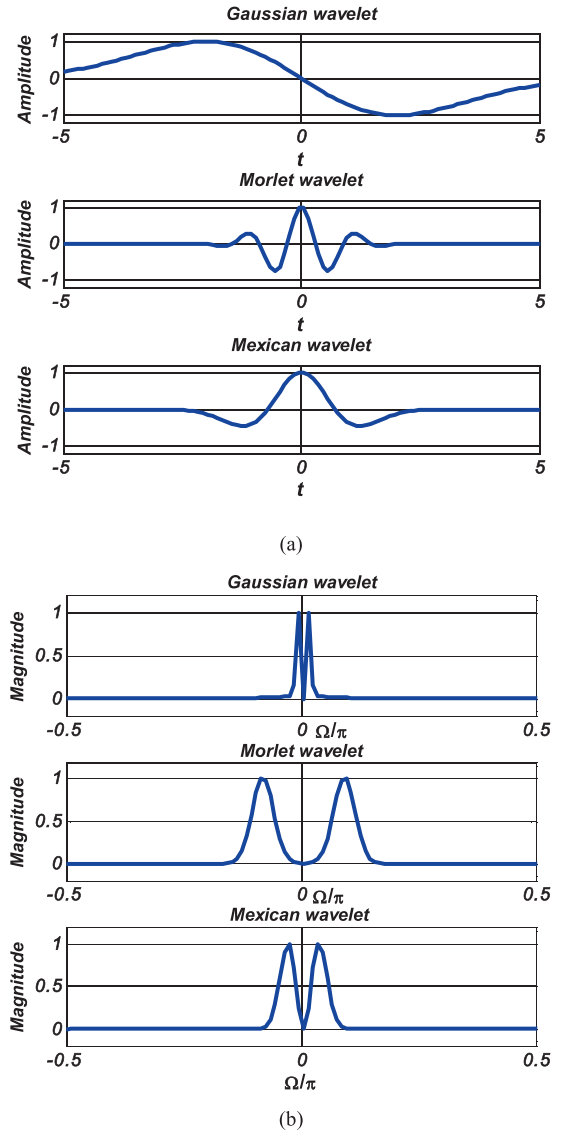


Fig. 2. Examples of mother wavelets functions (Gaussian wavelet, Morlet wavelet, and Mexican hat wavelet). (a) Time domain. (b) Frequency domain.

When finding an optimal scaling factor that satisfies (4) while changing  $s$ , the Gaussian wavelet will work quite well if the energy of an input signal is concentrated on a low frequency area, such as a baseband signal. On the other hand, the detection method using the Gaussian wavelet cannot distinguish the desired signal from the received signal when the operating frequency is high, as shown in Fig. 3(c). This is why  $s_{\text{opt}}$  has to be as small as possible to detect high-frequency components, but small  $s_{\text{opt}}$  also suppresses the input signal, resulting in a low SNR.

Moreover, there could also be several radar signals with different carrier frequencies. In this case, since the optimal scaling factor can be obtained only by (4), some of the signals may be missed if all components of the input signal with different frequencies may not be involved in the bandwidth, as shown in Fig. 3(d).

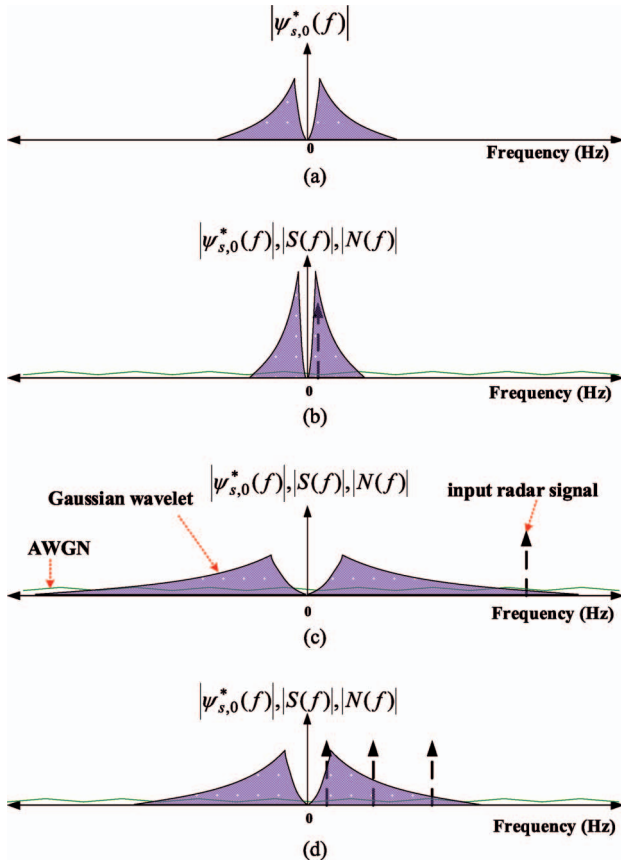


Fig. 3. Magnitude of FT when applying Gaussian wavelet to various signals. (a) Mother wavelet. (b) Input signal concentrated at low frequency. (c) Input signal with high operating frequency. (d) Input signal with multifrequency components.

### III. WEAK-SIGNAL DETECTION BASED ON THE MODIFIED SINC WAVELET

To overcome the limitation of needing prior knowledge, we propose a new wavelet-based weak-signal detection technique that can operate without any prior information about the signals. The method also works well even when the unknown signal has high-frequency components or multiple frequencies. This can be achieved through generation of a new wavelet function called a modified sinc wavelet.

#### A. Modified Sinc Wavelet

As shown in Fig. 3, high-frequency signals may not be effectively detected by conventional wavelet-based noise-reduction methods, even with the optimal scaling factor. In addition, to detect multifrequency component signals, a wavelet function should have a flat frequency response. The best solution may be to find an optimal mother wavelet function that is robust to any kind of signal. However, since this paper's main focus is on the practical use of the detection method, we do not deal with the optimal mother wavelet issue. Instead, a new wavelet function was designed to operate robustly for unknown

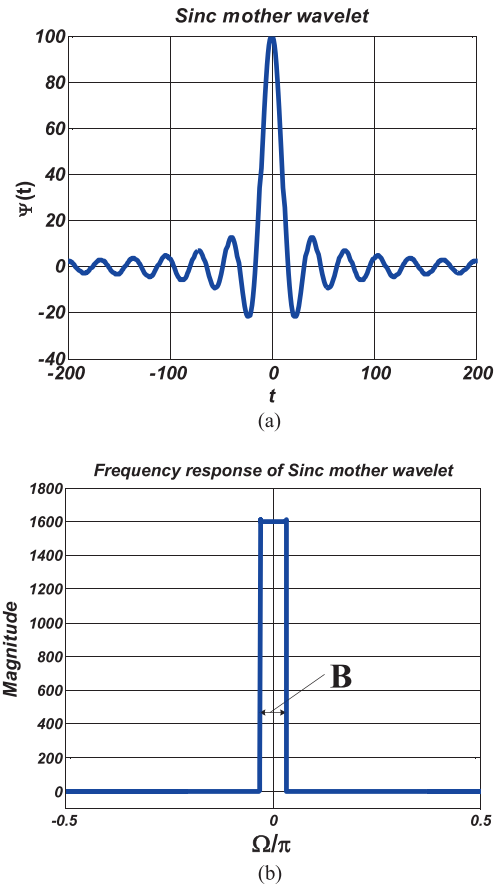


Fig. 4. Sinc function. (a) Time domain representation. (b) Frequency response.

signals with high-frequency or multifrequency components.

Fig. 4(a) shows the sinc function, which has a flat frequency response, in contrast to other wavelet functions. The sinc function is as follows:

$$\psi(t) = \frac{\sin(B\pi t)}{\pi t} \quad (5)$$

where  $B$  is the initial bandwidth of the filter, which can be set arbitrarily. To effectively manage various signals, we propose a sinc wavelet function with a variable center frequency. The frequency shifting can be achieved as follows [24]:

$$e^{j2\pi f_0 t} x(t) \xrightarrow{FT} X(j2\pi(f - f_0)). \quad (6)$$

Applying the property (6) to (5), the frequency variable wavelet function can be written as follows:

$$\begin{aligned} \psi_{s,0}^*(-b) &= e^{j2\pi f_0(b/s)} \frac{1}{\sqrt{|s|}} \frac{\sin[2\pi(B/2)b/s]}{\pi b/s} \\ &= \sqrt{s} e^{j2\pi(f_0/s)b} \frac{\sin[2\pi(Bs/2)b]}{\pi b}. \end{aligned} \quad (7)$$

Here,  $f_0/s$  denotes the variable center frequency of  $\Psi_{s,0}^*(f)$ , and the initial shifting value of  $f_0$  is selected by users. The



FT of (7) is as follows:

$$\Psi_{s,0}^*(f) = \begin{cases} \sqrt{s}, & \frac{f_0}{s} - \frac{B/s}{2} < f < \frac{f_0}{s} + \frac{B/s}{2} \\ 0, & \text{otherwise} \end{cases} \quad (8)$$

For a function to be a mother wavelet, it has to integrate to zero ( $\int_{-\infty}^{\infty} \psi(t)dt = 0$ ) and have finite energy ( $\int_{-\infty}^{\infty} |\psi(t)|^2 dt < \infty$ ). This is the admissibility condition, which is necessary to obtain the inverse from the CWT [8, 23].

The integral of a sinc function does not converge to zero:

$$\int_{-\infty}^{\infty} \text{sinc}(x)dx = \int_{-\infty}^{\infty} \frac{\sin(\pi x)}{\pi x} dx = 1. \quad (9)$$

Thus, this function cannot be a mother wavelet. However, the modified sinc wavelet shown in (7) satisfies this condition and can indeed be a mother wavelet with a constraint defined by the initial frequency and bandwidth. The integral of the modified sinc wavelet can be derived easily using the FT property of a sinc function:

$$\int_{-\infty}^{\infty} \frac{\sin(\pi t)}{\pi t} e^{-j2\pi f t} dt = \text{rect}(f) \quad (10)$$

where

$$\text{rect}(a) = \begin{cases} 1, & |a| \leq \frac{1}{2} \\ 0, & \text{otherwise.} \end{cases} \quad (11)$$

The modified sinc mother wavelet is defined as

$$\psi(t) = e^{-j2\pi f_0 t} \frac{\sin(\pi B t)}{\pi t}. \quad (12)$$

The integral of (12) is calculated using (10) as follows:

$$\int_{-\infty}^{\infty} \psi(t)dt = \int_{-\infty}^{\infty} \frac{\sin(\pi B t)}{\pi t} e^{-j2\pi f_0 t} dt. \quad (13)$$

Substituting  $t'$  for the variable  $Bt$ , (13) is rewritten as

$$\int_{-\infty}^{\infty} \frac{\sin(\pi t')}{\pi t'} e^{-j2\pi \frac{f_0}{B} t'} dt' = \text{rect}\left(\frac{f_0}{B}\right). \quad (14)$$

The modified sinc wavelet also has finite energy. Therefore, if we set the initial frequency and bandwidth as  $2f_0 > B$ , the modified sinc wavelet satisfies the admissibility condition. This result comes from the fact that the dc component ( $f = 0$ ) of the sinc function disappears by setting  $2f_0 > B$ .

From (8), changing  $s$  generates variation in the bandwidth and amplitude of  $\Psi_{s,0}^*(f)$ . The main achievement over the previous wavelet-based noise-reduction method is the variable center frequency. Shifting the center frequency is beneficial in weak radar signal detection for the following reason. If  $s < 1$ , the center frequency ( $f_0/s$ ) moves to the high-frequency band. When the operating frequency of the weak radar signal is quite high, the optimal scaling factor  $s_{opt}$  in the conventional wavelet-based method becomes too small, since the method changes only the scaling factor to find signal components. However, the center frequency shifting property of the proposed method makes it possible to

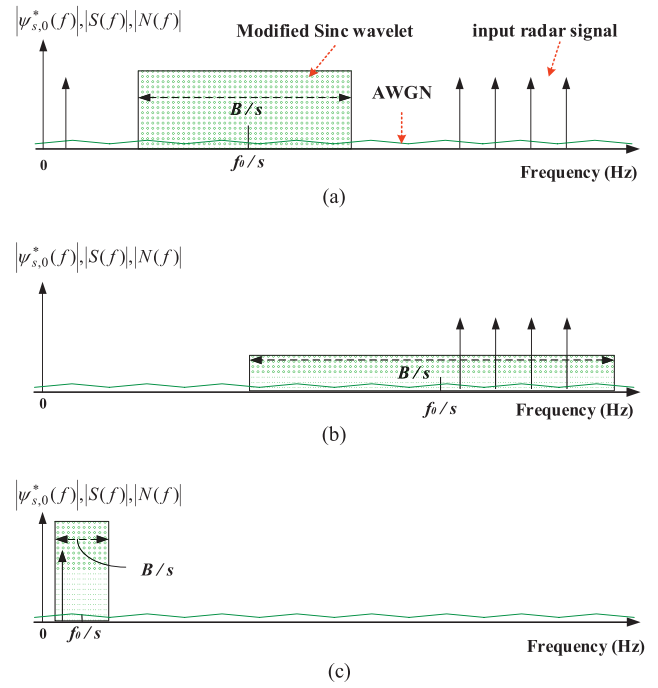


Fig. 5. Spectral view of proposed method. (a)  $s = 1$ ; (b)  $s < 1$ . (c)  $s > 1$ .

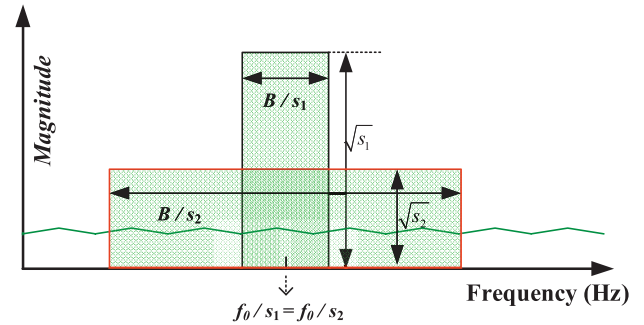


Fig. 6. Spectral view of frequency response of modified sinc wavelet, which has same center frequency with different bandwidth when aliasing occurs.

secure a larger value of  $s_{opt}$ , as shown in Figs. 5(a) and 5(b). The method also copes well with low operating frequency because the scaling factor  $s$  will be larger than 1 in such cases. Therefore, we can efficiently extract an enemy signal, as shown in Fig. 5(c).

Another advantage of using the modified sinc wavelet comes from the aliasing phenomenon induced by shifting the center frequency. Fig. 6 shows two band-pass filters with the same center frequency and different bandwidth generated by the same mother wavelet of the modified sinc wavelet. This phenomenon is expected for different scaling factors ( $s_1, s_2$ ):

$$2f_{\max} + \frac{f_0}{s_1} = \frac{f_0}{s_2} \rightarrow s_2 = s_1 \left( \frac{f_0}{2s_1 f_{\max} + f_0} \right), \quad (15)$$

where  $f_{\max}$  is the maximum frequency of a channel and the same as half of the sampling frequency. Therefore, using a modified sinc wavelet, multiple band-pass filters with different bandwidth and the same center frequency can be

implemented by only adjusting scaling factors, enabling both narrowband and wideband signal detections in a frequency region.

### B. Initial Setup of Frequency and Bandwidth

Choosing the initial values of  $f_0$  and  $B$  is very important because they can determine the performance of the whole detection process. For example, if the radar operating frequency is much higher than the initial frequency  $f_0$ , we may not expect an excellent advantage in terms of the SNR. When we decrease the scaling factor so that the center frequency approaches the desired band, the SNR decreases due to the enlarged bandwidth of the scaled wavelet function. In addition, the initial value of  $B$  is an important factor that controls the amount of noise flow in the passband. Before determining the specific values of  $f_0$  and  $B$ , the characteristics of the filter according to the variation of the scaling factor must be examined.

As shown in (7), the center frequency, bandwidth, and amplitude of the modified sinc wavelet are expressed as  $f_0/s$ ,  $B/s$ , and the square root of  $s$ , respectively. The bandwidth of the largest passband is determined by the minimum value of a scaling factor and cannot exceed the channel bandwidth  $B_{CH}$ . Assuming that a down-converted channel has a frequency range of  $[0 \text{ Hz}, B_{CH} \text{ Hz}]$ , the minimum value of a scaling factor  $s_{\min}$  can be obtained by

$$\frac{B}{s_{\min}} < B_{CH} \rightarrow s_{\min} > \frac{B}{B_{CH}}. \quad (16)$$

Here,  $s_{\min}$  can be selected by a proper value satisfying (16) and this value determines the maximum passband width of the modified sinc wavelet. On the other hand, the maximum value of the scaling factor  $s_{\max}$  is unrestricted because as the scaling factor increases without any bound, the center frequency of the scaled wavelet asymptotically approaches the minimum frequency (0 Hz) of the channel with bandwidth  $B/s_{\max}$ . However, since the initial values of  $f_0$  and  $B$  also affect the channel center frequency and bandwidth, determining the specific value of  $s_{\max}$  may not be a crucial task to describe the characteristics of the modified sinc wavelet. For example, if we want to set a filter having a center frequency  $f_k$ , the desired center frequency can be obtained from different combinations of an initial center frequency and a scaling factor such as  $(f_a, s_a)$  and  $(f_b, s_b)$ , which can be easily shown as follows:

$$f_k = \frac{f_a}{s_a} = \frac{f_b}{\left(f_b \cdot \frac{s_a}{f_a}\right)} = \frac{f_b}{s_b}, \quad (17)$$

where  $f_a > f_b$ ,  $s_a > 1$ , and  $s_b < 1$ . Therefore, we do not need an overly large value of  $s$  to make a highly narrow passband and low center frequency. Here, we just set  $s_{\max} = 1$  and then only focus on presenting the number of scaling factors and determination of initial values.

A candidate set of scaling factors can be determined by various methodologies. A simple method is to configure equally spaced  $s_i$  with the desired number of total scaling factors within the range of  $s_{\min} \leq s_i \leq 1$ .

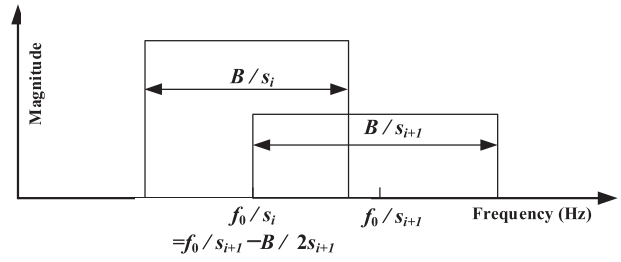


Fig. 7. Spectral view of frequency response of adjacent wavelets of modified sinc wavelet.

Otherwise, defining two adjacent values by  $s_i$  and  $s_{i+1}$ , we can set the adjacent scaled wavelets by overlapping half of the bandwidth, as shown in Fig. 7. The relation between  $s_i$  and  $s_{i+1}$  is determined by

$$\frac{f_0}{s_i} = \frac{f_0}{s_{i+1}} - \frac{B}{2s_{i+1}} \rightarrow s_{i+1} = s_i \left( \frac{2f_0 - B}{2f_0} \right) = \lambda s_i. \quad (18)$$

Based on (18), the choice of an initial frequency and bandwidth affects the number of filter banks generated by the modified sinc wavelet and the minimum passband width. A larger value of  $\lambda$  generates a larger number of filter banks and narrower passband widths.

Fig. 8 shows the shapes of filter banks of the modified sinc wavelet according to the different values of initial frequency ( $f_0$ ) and initial bandwidth ( $B$ ). Figs. 8(a) and 8(b) show the filter shapes of the modified sinc wavelet with  $f_0 = 2 \text{ kHz}$  and  $9 \text{ kHz}$ , respectively, and the same  $B$ . The higher initial center frequency of Fig. 8(b) provides a larger number of filter banks, which can deal with more types of incoming signals.

Figs. 8(c) and 8(d) show the filter shapes of the modified sinc wavelet with  $B = 1.5 \text{ kHz}$  and  $0.5 \text{ kHz}$ , respectively, and the same  $f_0$ . The narrower initial bandwidth of Fig. 8(d) provides a larger number of filter banks. Although the initial bandwidth is the same, Fig. 8(c) provides fewer filter banks to cover more types of incoming signals than Fig. 8(d). Moreover, Fig. 8(c) suffers from forming narrowband filters in the low frequency areas. Therefore, from Fig. 8 and (18), the high initial center frequency and narrow initial bandwidth that coincide with the small value of  $\lambda$  are favorable when using the modified sinc wavelet for robust weak signal detection.

### C. Block Diagram of Entire Procedure

A block diagram of the entire procedure is shown in Fig. 9. The proposed method is mainly divided into three parts: the channel selection, the estimation of an optimal scaling factor, and signal detection. The channel selection is firstly performed for each channel to find  $ch_{in}$  using a conventional channelized receiver, as shown in Fig. 10. The entire frequency band is divided into  $N$  subchannels with each bandwidth of  $B_{CH}$ . The signal in each channel is down-converted to the normalized frequency, and the power calculation of each channel is performed in this

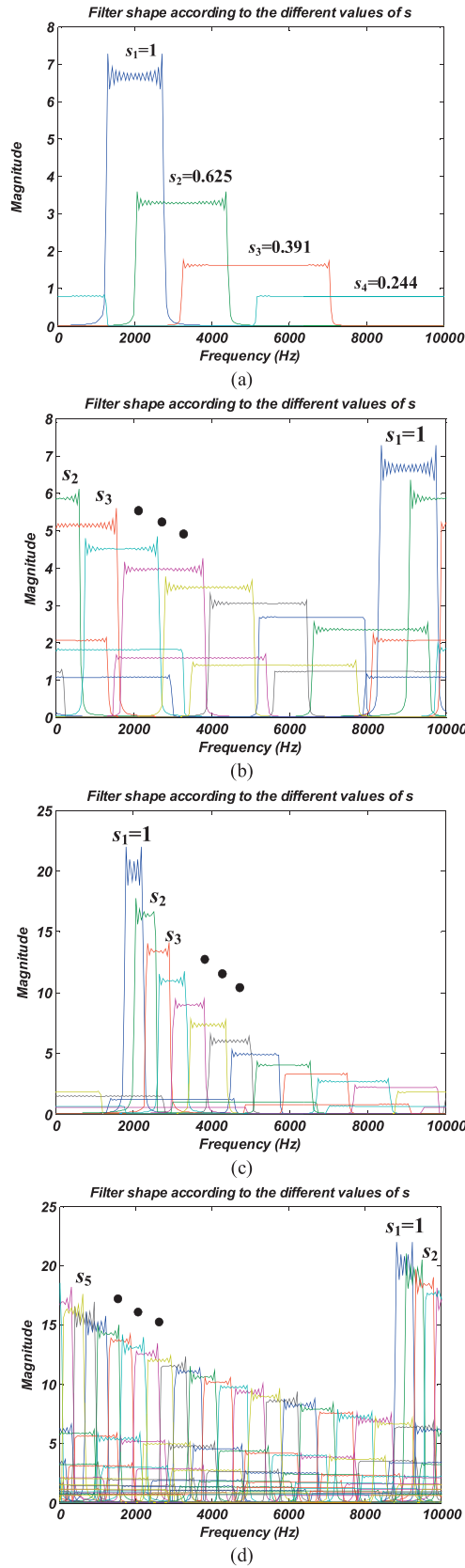


Fig. 8. Frequency response with values of different initial frequency ( $f_0$ ) and initial bandwidth ( $B$ ) when channel bandwidth ( $B_{CH}$ ) is 10 kHz. (a)  $f_0 = 2$  kHz and  $B = 0.5$  kHz. (b)  $f_0 = 9$  kHz and  $B = 1.5$  kHz. (c)  $f_0 = 2$  kHz and  $B = 0.5$  kHz. (d)  $f_0 = 9$  kHz and  $B = 1.5$  kHz.

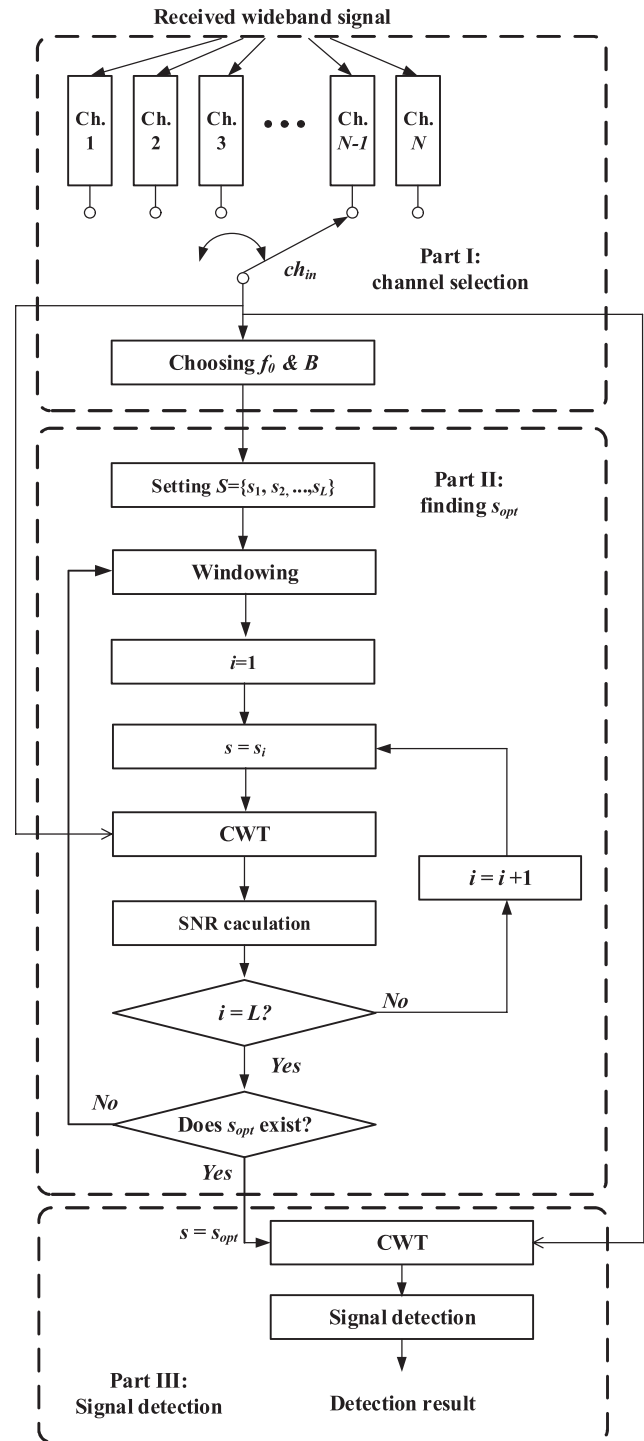


Fig. 9. Block diagram of entire procedure.

stage. The simplest way to determine the existence of enemy radar signals in each designated channel is to use the power measurement of a channelized signal:

$$P_i = \frac{1}{M} \sum_{m=1}^M y_{D,i}^2[m], \quad (19)$$

where  $M$  is the number of obtained samples. A channel containing the maximum power will be selected and used

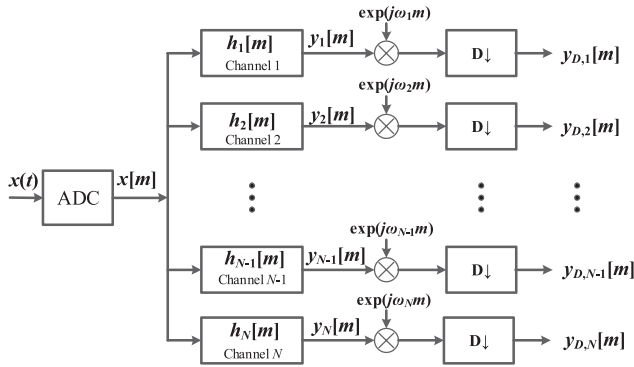


Fig. 10. Channelized receivers [25, 26].

for the detailed detection procedure using the modified sinc wavelet in the next stages.

In the second part, it is first necessary to determine a set of scaling factors,  $s = \{s_1 = 1, s_2, \dots, s_L = s_{\min}\}$ . The input signal from the selected  $ch_{in}$  is segmented using a simple rectangular window. Then, the CWT results of the input signal and the noise are independently calculated. Then, the power ratios between wavelet transformed signals are calculated according to the individual scaling factors and noise signal. A scaling factor that produces the highest power ratio will be selected as an optimal value. Note that the wavelet transform of the noise signal has to be performed using acquired signals beforehand under the assumption that the statistical properties of the noise signal do not change during the total acquisition time. In this case, it is possible to obtain samples of the noise signal from the surrounding environment without a target signal.

If there is no meaningful signal in the frame, the power ratio between the input signal and the noise in the transform domain will have similar values, regardless of the scaling factor  $s$ . Therefore, we determine that there is no desired signal in a frame segmented by a windowing process and then do the same process in the next frame. On the other hand, if the desired signal is included in the frame, the power ratio of the present frame will be dominant at a specific scaling factor, which will become  $s_{opt}$ . The detection process starts once  $s_{opt}$  is obtained. We assume that there always exists an optimal scaling factor and do not consider the determination algorithm. Finally, with the value of  $s_{opt}$  and the partitioned input signal, the wavelet transform is performed using the modified sinc wavelet as a final process.

#### IV. SIMULATION RESULTS

The proposed method was compared with Gaussian wavelet transform and conventional channelized receiver using computer simulations. The channel involving signal components was assumed to be successfully found by an initial channelization process in Part I of Fig. 9.

Two kinds of the modified sinc wavelets with different initial values were considered. The frequency response of the Gaussian mother wavelet is similar to that of other frequently used mother wavelets, such as the Morlet and

the Mexican hat shown in Fig. 2. Thus, we provide only the results of the Gaussian wavelet as a comparison target among several mother wavelet shapes. We also consider the modified Gaussian wavelet with frequency-shifted passband characteristics similar to the modified sinc wavelet. The conventional channelized receiver which has equal passband width for every subchannel was configured by using the frequency-shifted sinc functions for fair comparison in terms of frequency response. Note that this channelizer should be distinguished from the one that is used to find the initial channel in Part I of Fig. 9 despite the same structure. The number of channels of the channelized receiver was the same as the number of scaling factors. Therefore, the computational complexity was the same for each method.

The simulations were performed under conditions of an AWGN environment, and the received signals were modeled using a single narrowband signal, multiple narrowband signals, and linear frequency modulation (LFM) wideband signal. The bandwidth  $B_{CH}$  of the selected channel is 1 GHz. The initial center frequency of the modified sinc wavelet was 480 MHz, and the initial bandwidths were 28 MHz and 10 MHz. The number of filter banks for each detection method was 100, so the individual bandwidth of the channelized receiver was 20 MHz with an overlapping range of the individual half bandwidth. The specific value of the selected total channel bandwidth can be varied with the choice of the initial channelization process, and the initial values of the modified sinc wavelet are also affected by the determined channel bandwidth of channelization in Part I. The only effective parameter for determining the performance is the ratio between total bandwidth of the selected channel in the initial channel selection process and the bandwidth of a subband in detection process, and thus we chose a channel bandwidth of 1 GHz for simplicity. The simulation environments are summarized in Table I.

To evaluate the performance of the proposed method, let the  $i$ th channel be selected through the initial channelization process. Then, we denote the received signal of the  $i$ th selected channel as

$$y_{D,i}[m] = x_{D,i}[m] + n_i[m] \quad (20)$$

where  $x_{D,i}[m]$  is the down-converted radar signal and  $n_i[m]$  is the noise signal in  $i$ th channel. Then, we used an output SNR calculated by

$$SNR_{out} = 10 \log \left( \frac{\sum_{m=1}^K z_X^2[m]}{\sum_{m=1}^K z_N^2[m]} \right) \quad (21)$$

where  $K$  is the number of output samples. In addition,  $z_X[m]$  is the selected subband filter output of the down-converted radar signal  $x_{D,i}[m]$ , and  $z_N[m]$  is the selected subband filter output of the corresponding noise signal  $n_i[m]$ , in both cases of the channelized receiver and the wavelet transforms.



TABLE I  
The Parameters Used for Each Detection Method

		Detection Methods		
		Modified Sinc	Gaussian/ Modified Gaussian	Channelized Receiver
Initial values	$f_0 = 480$ MHz, $B = 28$ MHz	$f_0 = 480$ MHz, $B = 10$ MHz		Bandwidth = 20 MHz
Filter bank type	Overlap a half of adjacent filter banks	Equally spaced scaling factor	Equally spaced scaling factor	Overlap a half of adjacent filter banks
# of filter banks		100		

#### A. Single Narrowband Signal

A pulse sequence with unknown frequency is assumed to be received at the receiver, as shown in Fig. 11(a). The distorted weak signal of  $-5$  dB is represented in Fig. 11(b). Each pulse sequence was assumed to have the same narrowband frequency. The power ratio obtained from (4) with different scaling factors is shown in Fig. 11(c). Due to the variable bandwidth in one frequency region, there are several high power ratios. Among them, the narrowest band with the largest power ratio is selected as  $s_{\text{opt}}$ . The final transformed signal is depicted in Fig. 11(d).

The average output SNR of the modified sinc wavelet is compared with that of the Gaussian wavelet, modified Gaussian wavelet, and the channelizer according to the input SNR of the selected channel in Fig. 12. The frequency of the narrowband signal is randomly generated at each iteration within the range of total selected channel bandwidth. The modified sinc wavelet clearly outperforms the Gaussian wavelet-based signal detectors. This may have resulted from the fact that the Gaussian wavelet focuses on low-pass filtering, which leads to difficulty in detecting high-frequency signals. In addition, although the modified Gaussian wavelet applies the frequency shift property as in the modified sinc wavelet, the Gaussian wavelet forms a null shape at the center of its passband, as shown in Fig. 2. Therefore, it does not efficiently operate as a band-pass filter. When comparing the channelizers, the modified sinc wavelet using a 10 MHz initial bandwidth outperforms the channelized receiver. As mentioned in Section III-B, the shapes of each filter bank generated by the modified sinc wavelet are affected by the initial center frequency and bandwidth. Fig. 12 shows that the modified sinc wavelet outperforms the fixed channelized receiver when choosing an appropriate initial center frequency and bandwidth.

#### B. Multiple Narrowband Signals and Wideband Signal

In the simulation of multiple narrowband source signals, 4 frequency components were considered (100 MHz, 120 MHz, 150 MHz, and 200 MHz). Each single source is assumed to be received as a part of the pulse sequence. Therefore, a total of 4 pulses are considered to generate a pulse sequence. Fig. 13 compares the average output SNR for multiple source signals. The detection performance is similar to the case of a single narrowband

source signal. However, if the individual frequencies are far away from each other, the modified sinc wavelet may choose a scaling factor that produces wide bandwidth. This causes a decrease in SNR. Otherwise, the modified sinc wavelet will choose a scaling factor that produces narrow bandwidth that gives up a part of the multiple signal components. This phenomenon also occurs in other detection methods.

In a single wideband signal simulation, an LFM waveform with random center frequency and 100 MHz bandwidth is assumed to be received as a pulse sequence, as shown in Fig. 11(a). This bandwidth is too large and thus seems impractical. However, the LFM is a representative waveform of a wideband signal [28], and thus we tried to generate a wideband signal example through the LFM waveform. Fig. 14 shows the output SNR comparison results for a single wideband source signal. The modified sinc wavelet outperforms the Gaussian wavelet-based detectors and shows a similar output power to the channelized receiver. It seems that the channelized receiver outperforms the modified sinc wavelet. However, this result comes from the insufficient passband width of the designed channelized receiver compared with the proposed method. Even though output SNR performance is secured, this would cause a partial loss of the original source signal information and may thus prevent exact estimation of signal parameters such as PW or PRI in ES systems.

In these simulations, the modified sinc wavelet shows remarkable performance enhancement compared with the Gaussian wavelet-based detection algorithms. In addition, it shows similar or better detection performance to a fixed channelized receiver that is also configured using the sinc wavelet transform under the assumption of the same number of filter banks and computational complexity. As a result, the modified sinc wavelet can be a good candidate for making digital filter banks using only a mother wavelet function and a set of scaling factors in a weak-signal detection problem.

#### V. CONCLUSION

We have proposed a new wavelet-based weak signal detection method using a modified sinc mother wavelet to deal with unknown low-SNR signals. The proposed method changes the center frequency and the bandwidth

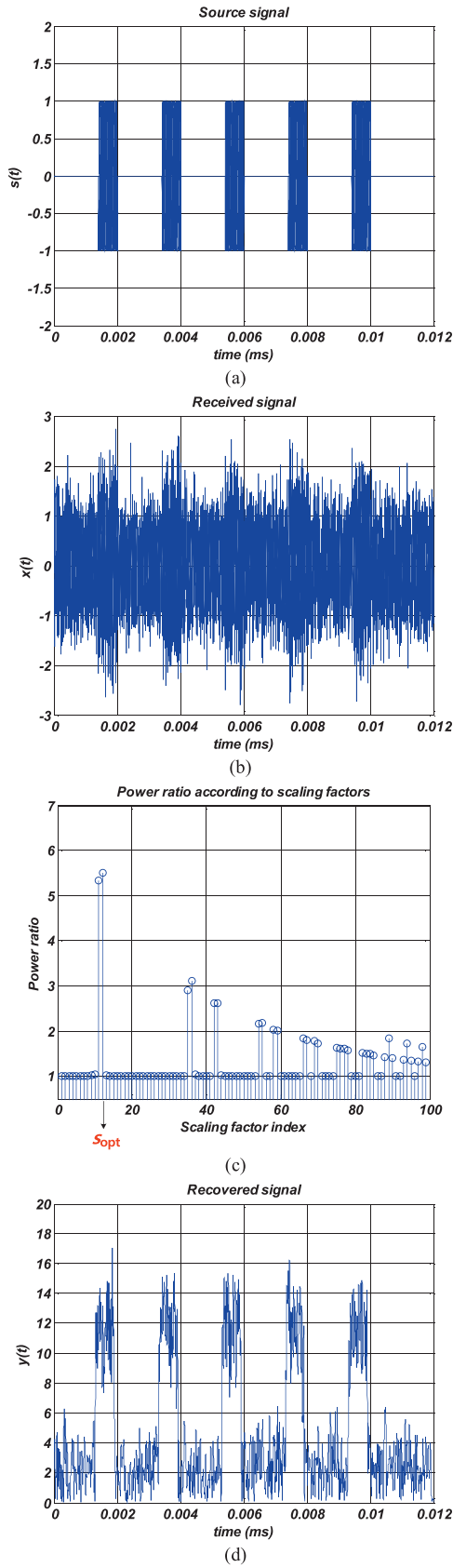


Fig. 11. Operation of modified sinc wavelet. (a) Original pulse sequence. (b) Distorted pulse sequence ( $-5$  dB). (c) Ratio according to scaling factor. (d) Transformed output.

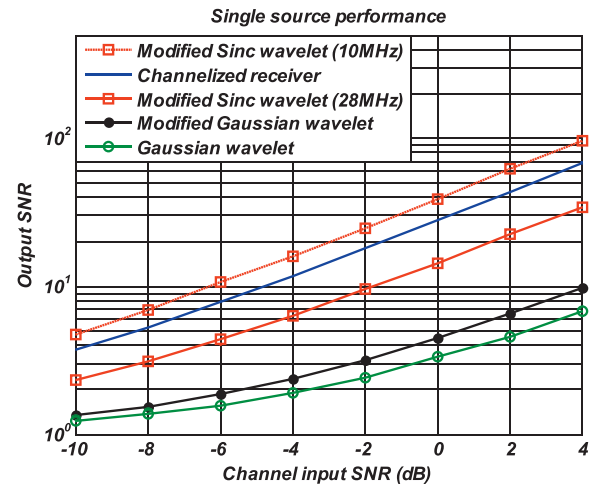


Fig. 12. Output SNR comparison for detection of single narrowband source signal (random frequency).

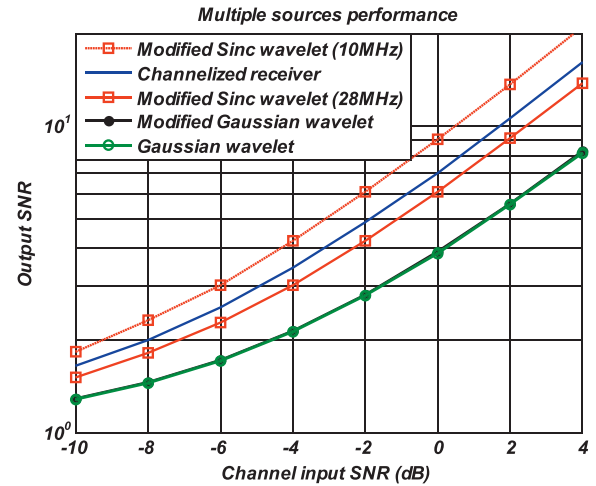


Fig. 13. Output SNR comparison for detection of multiple source signals (100 MHz, 120 MHz, 150 MHz, 200 MHz).

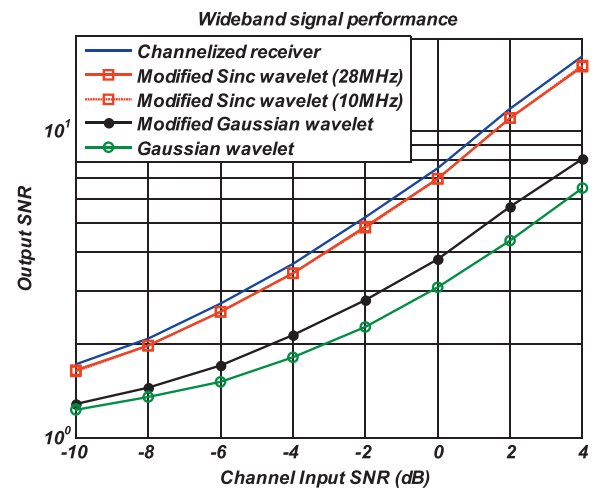


Fig. 14. Output SNR comparison for detection of single wideband source signal (random center frequency and 100 MHz bandwidth).

by adjusting the optimal scaling factor, which makes it flexible in responding to unknown weak radar signals. A weak signal detector based on this method showed large SNR enhancement compared with the conventional wavelet-based detectors and moderate performance enhancement compared with a channelized receiver. Due to the flat gain of the modified sinc wavelet, the method worked well when detecting unknown weak signals with high frequency or wide bandwidth. Therefore, the method is expected to contribute to the performance improvement of ES systems, especially in solving weak-signal detection problems caused by a lack of information about the threatening radar signals and power attenuation due to long distances from the signal sources.

## REFERENCES

- [1] David, L. A.  
*EW 101: A First Course in Electronic Warfare*. Norwood, MA: Artech House, 2003.
- [2] David, L. A.  
*EW 103: Tactical Battlefield Communications Electronic Warfare*. Norwood, MA: Artech House, 2009.
- [3] Skolnik, Merrill I.  
*Introduction to Radar Systems*, 2nd ed. New York: McGraw-Hill, 1980.
- [4] Skolnik, Merrill I.  
*Radar Handbook*, 2nd ed. New York: McGraw-Hill, 1990.
- [5] Wiley, R. G.  
*Electronic Intelligence: The Analysis of Radar Signals*, 2nd ed. Norwood, MA: Artech House, 1993.
- [6] David, L. A.  
*Introduction to Electronic Warfare Modeling and Simulation*. Norwood, MA: Artech House, 2003.
- [7] Cui, G., Liu, J., Li, H., and Himed, B.  
Target detection for passive radar with noisy reference channel.  
*In Proceedings of IEEE Radar Conference*, Cincinnati, OH, 2014, 144–148.
- [8] Ehara, N., Sasase, I., and Mori, S.  
Weak radar signal detection based on wavelet transform.  
*In Proceedings of IEEE International Conference on Acoustics, Speech, and Signal Processing (ICASSP)*, Adelaide, SA, 1994, 377–380.
- [9] Rong, H., Jin, W., and Zhang, C.  
Application of support vector machines to pulse repetition interval modulation recognition.  
*In Proceedings of 6th International Conference on ITS Telecommunications*, Chengdu, China, 2006, 1187–1190.
- [10] Xin, Y., Xiang, Z., Dong, L., Zhu, B., Cao, H., and Fang, Y.  
A center frequency adjustable narrow band filter for the detection of weak single frequency signal.  
*Review of Scientific Instruments*, **85**, 4 (Apr. 2014), 1164–1168.
- [11] Wang, J., Yang, L., Gao, L., and Miao, Q.  
Current progress on weak signal detection.  
*In Proceedings of International Conference on Quality, Reliability, Risk, Maintenance, and Safety Engineering (QR2MSE)*, Chengdu, China, 2013, 1812–1818.
- [12] Visnevski, N., Haykin, S., Krishnamurthy, V., Dilkes, F. A., and Lavoie, P.  
Hidden Markov models for radar pulse train analysis in electronic warfare.  
*In Proceedings of IEEE International Conference on Acoustics, Speech, and Signal Processing (ICASSP)*, 2005, 597–600.
- [13] Rogers, J. A. V.  
ESM processor system for high pulse density radar environments.  
*IEEE Proceedings – F, Communications, Radar & Signal Processing*, **132**, 7 (Dec. 1985), 621–625.
- [14] Shin, W. H., and Lee, W. D.  
A novel method for radar pulse tracking using neural networks.  
*In Proceedings of IEEE Symposium Electromagnetic Compatibility, 2003 (EMC 2003)*, Vol. 1, 2003, 543–546.
- [15] Wang, Y., Pan, Q., Yang, Y., and Miao, Z.  
Analysis of radar type recognition based on decision fusion.  
*In Proceedings of Intelligent Control and Automation, 2006 (WCICA 2006)*, Vol. 2, Dalian, China, June 2006, 6536–6539.
- [16] Tang, J., Yang, Z., and Cai, Y.  
Wideband passive radar target detection and parameters estimation using wavelets.  
*In Proceedings of IEEE International Radar Conference*, May 2000, 815–818.
- [17] Soon, I. Y., and Koh, S. N.  
Speech enhancement using 2-D Fourier transform.  
*IEEE Transactions on Speech and Audio Processing*, **11**, 6 (Nov. 2003), 717–724.
- [18] Sudha, S., Suresh, G. R., and Sukanesh, R.  
Wavelet based image denoising using adaptive thresholding.  
*In Proceedings of International Conference on Computational Intelligence and Multimedia Applications*, Vol. 3, Dec. 2007, 296–300.
- [19] Eom, I. K., and Kim, Y. S.  
Wavelet-based denoising with nearly arbitrarily shaped windows.  
*IEEE Signal Processing Letters*, **11**, 12 (Dec. 2004), 937–940.
- [20] Kim, Y.-H., Song, K.-H., Han, J.-W., and Kim, H.-N.  
Radar scan pattern analysis for reduction of false identification in electronic warfare support systems.  
*IET Radar, Sonar & Navigation*, **8**, 7 (Aug. 2014), 719–728.
- [21] Deng, N., and Jiang, C.-S.  
Selection of optimal wavelet basis for signal denoising.  
*In Proceedings of 9th International Conference on Fuzzy Systems and Knowledge Discovery (FSKD)*, Sichuan, China, 2012, 1939–1943.
- [22] Weiss, L. G.  
Wavelets and wideband correlation processing.  
*IEEE Signal Processing Magazine*, **11**, 1 (Jan. 1994), 13–32.
- [23] Rao, R. M., and Bopardikar, A. S.  
*Wavelet Transforms: Introduction to Theory and Application*. Reading, MA: Addison-Wesley, 1998.
- [24] Oppenheim, A. V., and Willsky, A. S.  
*Signals & Systems*, 2nd ed. Upper Saddle River, NJ: Prentice-Hall International, 1997.
- [25] Namgoong, W.  
A channelized digital ultrawideband receiver.  
*IEEE Transactions on Wireless Communication*, **2**, 3 (May 2003), 502–510.
- [26] Wang, Z., and Ji, L.  
Radar signal interception receiver based on digital channelizer.  
*In Proceedings of IEEE 11th International Conference on Signal Processing*, Beijing, China, 2012, 1764–1767.
- [27] Yoon, K.-S., Kim, W.-J., Song, K.-H., and Kim, H.-N.  
Denoising method for weak-power radar signals using the modified sinc wavelet.  
*In Proceedings of IEEE Military Communications Conference. MILCOM*, Boston, MA, Oct. 2009.
- [28] Richards, M. A.  
*Fundamentals of Radar Signal Processing*. New York: McGraw-Hill, 2005.



**Jong-Woo Shin (M' 15)** received the B.S. and M.S. degrees in electronic and electrical engineering from Pusan National University, Busan, Korea, in 2010 and 2012, respectively.

He is currently working toward the Ph.D. degree at the Communications and Signal Processing Laboratory (CSPL), Department of Electrical & Computer Engineering at Pusan National University, Busan, Korea. His main research interests are in the area of radar/sonar signal processing, digital signal processing, and array signal processing. He is a member of IEEE.



**Kyu-Ha Song** received the B.S. degree in electrical engineering from Kyungpook National University, Daegu, Korea, in 1996 and the M.S. degree in electrical engineering from Pohang University of Science and Technology (POSTECH), Pohang, Korea, in 1998, respectively.

Since 1998, he has been a principal researcher at the 2<sup>nd</sup> R&D institute 2<sup>nd</sup> Directorate, Agency for Defense Development, Daejeon, Korea, where he is currently working on research and development for defense systems. In 2012, he entered POSTECH, where he is currently working towards the Ph.D. degree. His research interests are signal processing, geo-location, and pattern recognition.



**Kyoung-Sik Yoon** received the B.S. and M.S. degrees from the Department of Electrical and Computer Engineering from Pusan National University (PNU), Pusan, Korea, in 2008 and 2010, respectively.

In 2010, he joined the Next Generation Product R&D center of Samsung Electronics developing the latest Samsung smart phone. His interests are the enhancement of RX sensitivity, the reduction of current consumption of smart phones, and the various RF calibration solutions for mass production.





**Hyoung-Nam Kim (M'00)** received the B.S., M.S., and Ph.D. degrees in electronic and electrical engineering from Pohang University of Science and Technology (POSTECH), Pohang, Korea, in 1993, 1995, and 2000, respectively.

From May 2000 to February 2003, he was with Electronics and Telecommunications Research Institute (ETRI), Daejeon, Korea, developing advanced transmission and reception technology for terrestrial digital television. In 2003, he joined the faculty of the Department of Electronics Engineering at Pusan National University (PNU), Busan, Korea, where he is currently a full professor. From February 2009 to February 2010, he was with the Department of Biomedical Engineering, The Johns Hopkins University School of Medicine, as a visiting scholar. From September 2015 to August 2016, he was a visiting professor at the School of Electronics and Computer Engineering, University of Southampton, UK. His research interests are in the area of digital signal processing, radar/sonar signal processing, adaptive filtering, and bio-medical signal processing, in particular, signal processing for digital communications, electronic warfare support systems, and brain-computer interface.

Dr. Kim is a member of IEEE, IEEK, and KICS.